

# Analysis of the Statistical Distribution of Energization Overvoltages of EHV Cables and OHLs

T. Ohno, A. Ametani, C. L. Bak, W. Wiechowski, and T. K. Sørensen

**Abstract--** Insulation levels of EHV systems have been determined based on the statistical distribution of switching overvoltages since 1970s when the statistical distribution was found for overhead lines. Responding to an increase in the planned and installed EHV cables, the authors have derived the statistical distribution of energization overvoltages for EHV cables and have made clear their characteristics compared with those of the overhead lines. This paper identifies the causes and physical meanings of the characteristics so that it becomes possible to use the obtained statistical distribution for the determination of insulation levels of cable systems.

**Keywords:** EHV cable, insulation coordination, energization overvoltage, modal theory.

## I. INTRODUCTION

THE statistical distribution of switching overvoltages has long been used for determining insulation levels of EHV systems since it was derived in 1970s for EHV overhead lines (OHLs) [1]–[4]. With an increase in the number of planned and installed EHV cables, it has become possible and necessary to obtain the statistical distribution of switching overvoltages for EHV cables using the physical and electrical data of these cables.

The authors have derived the statistical distribution of energization overvoltages of EHV cables through a number of computer simulations in PSCAD® [5]. Ten types of EHV cables and OHLs were studied in order to derive the statistical distribution of the switching overvoltages. In addition, different line lengths and feeding networks (source impedance values) were considered as parameters for each type of EHV cables and OHLs.

Characteristics of the statistical distributions were found through comparison of the statistical distributions of EHV cables and OHLs. In particular, it has been found that energization overvoltages for cables are lower than those for

OHLs with respect to maximum, 2 %, and mean values. Also, the effects of line lengths and feeding networks were found to be different for cables and OHLs.

Reference [5] discusses possible causes that can lead to the characteristics, but the discussions were limited to qualitative analyses. This paper identifies causes and physical meanings of the characteristics so that it becomes possible to use the obtained statistical distribution for the determination of insulation levels of cable systems. Section II summarizes the characteristics of the statistical distribution. Sections III – V discuss each characteristic by analyzing voltage waveforms of energization overvoltages. Finally, the conclusion is given in Section VI.

## II. CHARACTERISTICS OF THE STATISTICAL DISTRIBUTION

Reference [5] studied the energization overvoltages of EHV OHLs and cables based on data from 10 planned or existing lines, respectively. Four line lengths and four feeding networks were considered as parameters. These parameters were varied in a reasonable range as shown in Table 1. The source impedance of 1 mH was included for two reasons. The first reason is that effects of a steep initial voltage rise which is expected in the line energization from a distributed parameter source can be analyzed by it. The second reason is that a very small source impedance is often selected for the analysis of OHLs in order to find the most severe overvoltages, and therefore it was assumed that the same approach applied for cables would give most severe overvoltages as well.

TABLE I  
STUDY CONDITIONS AND PARAMETERS

Line length	24, 48, 72, and 96 km
Feeding network	1, 15, 30, and 100 mH (corresponds to fault current of 735, 49, 25, and 7 kA at 400 kV)

The simulations were performed 200 times with random switches under each study condition. In the study the following main characteristics of the statistical distribution was found:

- Energization overvoltages for cables are lower than those for OHLs with respect to maximum, 2 %, and mean values.
- Energization overvoltages for cables do not show any dependence on the line length while those for OHLs peak with a line length of 72 km.
- Energization overvoltages for cables become lower for a

---

T. Ohno is with Tokyo Electric Power Company, Tokyo, Japan (e-mail: ohno.teruo@tepcoco.jp, phone no. +81-3-6373-3738).

A. Ametani is with Doshisha University, Kyoto, Japan (e-mail: aametani@mail.doshisha.ac.jp).

C. L. Bak is with the Department of Energy Technology, Aalborg University, Aalborg, Denmark (e-mail: clb@et.aau.dk).

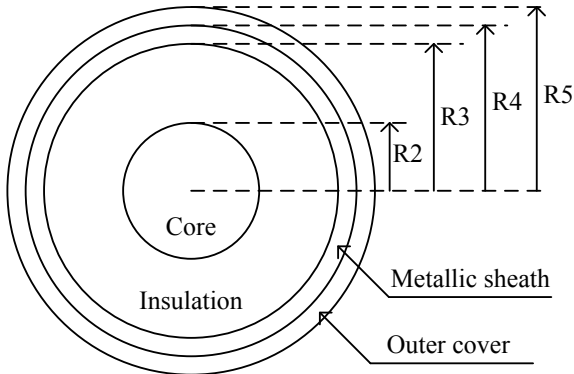
W. Wiechowski is with RWE Innogy, Swindon, United Kingdom (e-mail: wojciech.wiechowski@rwe.com)

T. K. Sørensen is with Energinet.dk, Fredericia, Denmark (e-mail: tks@energinet.dk).

Paper submitted to the International Conference on Power Systems Transients (IPST2013) in Vancouver, Canada, July 18-20, 2013

larger source impedance while those for OHLs peak with the source impedance 30 mH.

This paper focuses on the identification of causes and physical meanings for these three main characteristics. The analysis in this paper shows only one of 10 OHLs and one of 10 cables because the same characteristics and contributing factors were found in all OHLs and cables. The physical and electrical data of the selected 400 kV cable is shown in Fig. 1. The cable was modeled with frequency-dependent model in the phase domain in PSCAD [6].



R2 = 3.26cm, R3 = 6.14cm, R4 = 6.26cm, R5 = 6.73cm  
 Core inner radius: 0.0cm, Core resistivity:  $1.724 \times 10^{-8} \Omega\text{m}$ ,  
 Metallic sheath resistivity:  $2.840 \times 10^{-8} \Omega\text{m}$ ,  
 Relative permittivity (XLPE, PE): 2.4

Fig. 1 Physical and electrical data of the cable.

The cable was assumed to be directly buried at a depth of 1.3 m with a horizontal separation of 0.3 m as shown in Fig. 2. The cross-bonding diagram of the cable is shown in Fig. 3.

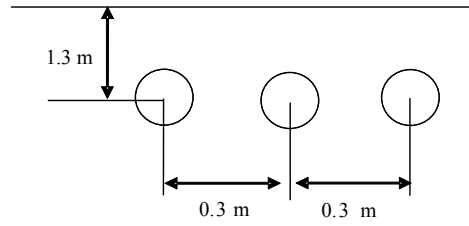


Fig. 2 Cable layout.

Key parameters of the selected 400 kV OHL are summarized in Table 2.

TABLE II  
 KEY PARAMETERS OF THE SELECTED OHL

Phase conductor	Martin
# of conductors in a bundle	2
Conductor separation [cm]	40
Resistance per conductor [ $\Omega/\text{km}$ ]	0.04259
Layout, top phase (X, Y) [m]	( $\pm 6.65, 34$ )
Layout, middle phase (X, Y) [m]	( $\pm 8.60, 26$ )
Layout, bottom phase (X, Y) [m]	( $\pm 7.10, 20$ )
Ground wire	68 / 138 AL
Resistance per conductor [ $\Omega/\text{km}$ ]	0.208
# of ground wires	2
Layout (X, Y) [m]	( $\pm 3.00, 41$ )

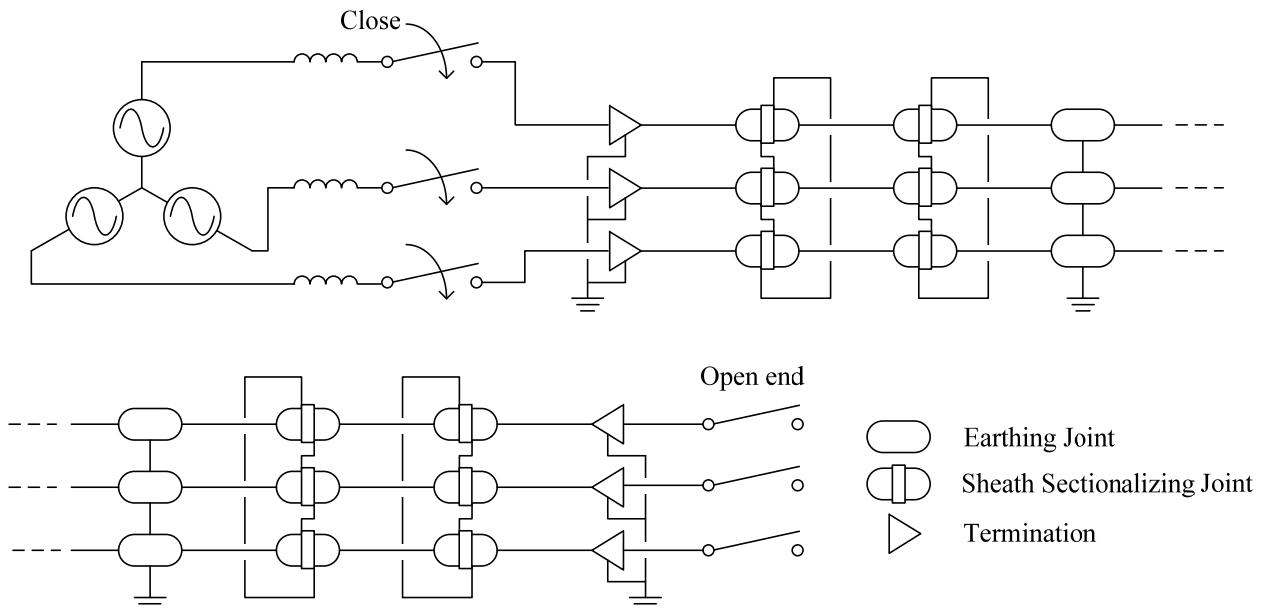


Fig. 3 Cross-bonding diagram of the selected cable.

Shunt reactors were directly connected to the cable at both ends when the line length was 24, 48, or 72 km. The compensation rate was set to 100 % so that only the transient component of the energization overvoltage can be observed. With the line length of 96 km, the shunt reactors were additionally connected to the center of the line. Necessary capacity of shunt reactors for 100 % compensation was shared by shunt reactors at both line ends and at the center with the proportions of 1/4, 1/4, and 1/2.

Charging capacity of the OHL was also compensated to 100 % in order to set the same condition as the cable. However, it is already known that the compensation does not have a noticeable impact on the energization overvoltage of the OHL [5].

### III. ANALYSIS OF THE HIGHEST OVERVOLTAGES

This section analyzes why energization overvoltages for cables are lower than those for OHLs with respect to maximum, 2 %, and mean values. This is achieved by analyzing voltage waveforms of energization overvoltages. Here, we define the maximum overvoltage as the largest overvoltage found in 200 random simulations.

Fig. 4 shows initial voltage waveforms of the energization overvoltage at the receiving end ( $V_r$ ) and at the sending end ( $V_s$ ) in phase a for one of 10 OHLs. The OHL was energized at the voltage peak of phase a (5 ms), and the voltage waveforms of phase a are shown in Fig. 4. The line length and the source impedance were fixed to 48 km and 30 mH, respectively.

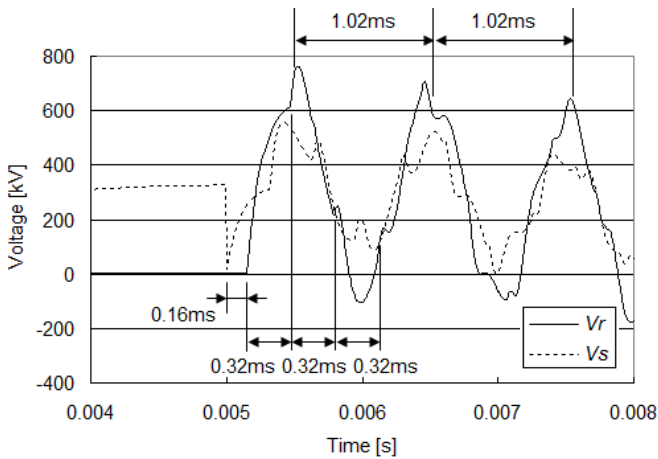


Fig. 4 Initial voltage waveforms of the energization overvoltage for an OHL (line length: 48 km, source impedance: 30 mH).

For the OHL, the overvoltage of the inter-phase mode travels at the speed of light. It arrives at the receiving end 0.16 ms ( $= 48 \text{ km} / 300 \text{ m}/\mu\text{s}$ ) after it departs from the sending end (1st wave).

The inter-phase mode is reflected back to the sending end, but  $V_r$  rises towards around 2 pu as the overvoltage of the earth-return mode arrives. The propagation time of the earth-return mode can be obtained by performing a frequency scan

on the energized system or by performing a Fourier transform of the voltage waveform. The result of the frequency scan shows the dominant frequency 980 Hz, which corresponds to the cycle time 1.02 ms. The result is realistic as Fig. 4 shows the voltage peak of the earth-return mode with an interval of 1.02 ms.

The initial voltage rise time at the receiving end is difficult to find theoretically since the initial voltage waveform does not follow the sinusoidal wave. The receiving end voltage starts to rise at 5.16 ms. Looking at the voltage amplitude of the earth-return mode, the voltage starts to rise from near the minimum. It suggests that it takes about 0.51 ( $= 1.02 / 2$ ) ms to reach the maximum of the earth-return mode, but Fig. 4 shows the earth-return mode reaches its maximum in approximately 0.32 ms after it starts to rise.

This can be explained by the rate of voltage rise. When the voltage starts from the minimum, the rate of the voltage rise should increase in the first 0.255 ( $= 1.02 / 4$ ) ms and should decrease in the remaining 0.255 ( $= 1.02 / 4$ ) ms, assuming the receiving end voltage follows the sinusoidal wave. However, in Fig. 4, the rate of voltage rise is largest when the receiving end voltage starts to rise. This makes the voltage rise time to 2 pu shorter, and the earth-return mode reaches its maximum in approximately 5.48 ( $= 5.16 + 0.32$ ) ms.

This reduction of the voltage rise time affects the magnitude of the highest overvoltage since 5.48 ms is exactly when the inter-phase mode comes back to the receiving end (2nd wave). As shown in Fig. 4, the inter-phase mode comes back to the receiving end with an interval of 0.32 ms as it travels at the speed of light. Since the peak of the earth-return mode (1st wave) and the peak of the inter-phase mode (2nd wave) reach their maximum almost at the same time, around 5.48 ms,  $V_r$  goes above 2 pu and reaches to 2.3 pu.

The same analysis on the initial voltage waveforms is performed for one type of underground cables. Fig. 5 shows initial voltage waveforms of the energization overvoltage at the receiving end ( $V_r$ ) and at the sending end ( $V_s$ ). Study conditions, such as the switch timing (5 ms), line length (48 km) and source impedance (30 mH), are kept equal to the study on the OHL.

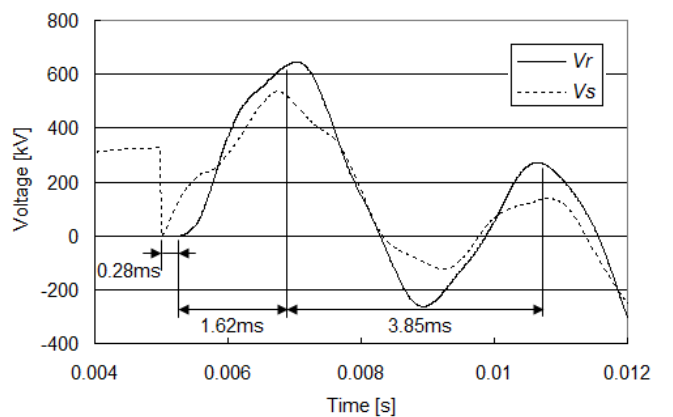


Fig. 5 Initial voltage waveforms of the energization overvoltage for a cable (line length: 48 km, source impedance: 30 mH).

In case of the underground cable, the overvoltage of the coaxial mode first arrives at the receiving end (1st wave). When a cable is not cross-bonded, the coaxial mode travels at

$$\frac{300}{\sqrt{\varepsilon_i}} = \frac{300}{\sqrt{2.852}} = 178 \text{ m}/\mu\text{s} \quad (1)$$

Here,  $\varepsilon_i$  is the relative permittivity of the insulation, which is converted to account for semiconductive layers (as described in [7]).

Since it is known that the propagation velocity is decreased for a cross-bonded cable [8], the propagation velocity is derived from the propagation time. Fig. 5 shows the coaxial mode (1st wave) arrives at the receiving end 0.28 ms after it leaves the sending end. The propagation velocity is calculated as 171 m/ $\mu$ s (= 48 km / 0.28 ms). The reduction of 7 m/ $\mu$ s or 3.5 % is a typical value [8].

Similarly to the OHL, the coaxial mode is reflected back to the sending end, but  $V_r$  rises towards around 2 pu as the overvoltage of the inter-phase mode arrives. The propagation time of the inter-phase mode can be obtained by performing a frequency scan on the energized system or by performing a Fourier transformation of the voltage waveform. The result of the frequency scan shows the dominant frequency 260 Hz, which corresponds to the cycle time 3.85 ms. The result is reasonable as Fig. 5 shows the voltage peak of the inter-phase mode with an interval of 3.85 ms.

The modes found in the energization overvoltage of the OHL and the cable are summarized in Table 3.

TABLE III  
DOMINANT MODE AND SUPERIMPOSED MODE  
OF THE ENERGIZATION OVERVOLTAGE

	OHL	Underground cable
Dominant mode (cycle time)	Earth-return mode (1.02 ms)	Inter-phase mode (3.85 ms)
Superimposed mode (propagation time)	Inter-phase mode (0.16 ms)	Coaxial mode (0.28 ms)

Now, comparing the initial voltage waveforms of the OHL and the cable, the superimposition of two different modes found in the OHL cannot be observed clearly in the cable. There are some distortions of voltage waveforms on the inter-phase mode caused by the coaxial mode, but the distortions only have a small contribution on the highest overvoltage. This is because the overvoltage of the coaxial mode is smaller and more obtuse, compared with the inter-phase mode in the OHL.

Another factor affecting the difference in the highest overvoltage is the long cycle time of the inter-phase mode in the cable. About the time when the inter-phase mode reaches its maximum (1st wave), the 4th wave of the coaxial mode arrives at the receiving end. At this time, the coaxial mode is

highly damped and is difficult to observe. Even in the OHL, the inter-phase mode can have an impact on the highest overvoltage only until its 2nd wave. It is highly damped and is difficult to observe after the 3rd wave.

#### IV. ANALYSIS ON THE EFFECTS OF LINE LENGTH

This section analyzes why energization overvoltages for cables do not show any dependence on the line length while those for OHLs peak with the line length 72 km.

Fig. 6 shows initial voltage waveforms of energization overvoltages of the OHL at the receiving end ( $V_r$ ). The switch timing is set to 5 ms as in the last section. The source impedance is set to 30 mH since the maximum overvoltage was observed with the source impedance 30 mH.

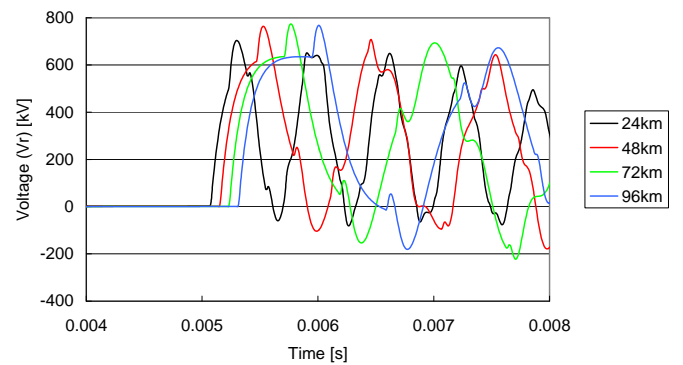


Fig. 6 Initial voltage waveforms of the energization overvoltage for the OHL (source impedance: 30 mH).

Fig. 6 demonstrates that highest overvoltages are caused by the superimposition of the earth-return mode (1st wave) and the inter-phase mode (2nd wave), regardless of the line length. However, depending on the line length, the inter-phase mode (2nd wave) comes back to the receiving end at different points-on-wave of the earth-return mode (1st wave). For example, when the line length is 24 km, the inter-phase mode (2nd wave) comes back to the receiving end before the earth-return mode (1st wave) reaches its maximum. As a result, the highest overvoltage becomes lower when the line length is 24 km. When the line length is 72 km, the inter-phase mode (2nd wave) comes back to the receiving end exactly when the earth-return mode (1st wave) reaches its maximum. This is why energization overvoltages of OHLs peak with the line length 72 km.

It has been shown that, for the source impedance 30 mH, the line length 72 km leads to the highest overvoltage. Considering how highest overvoltages are caused, different line lengths should lead to the highest overvoltage for different source impedances. For example, when the source impedance is 100 mH, the cycle time of the dominant overvoltage becomes larger. Therefore, a longer line length, which requires longer propagation time, should lead to the highest overvoltage.

Fig. 7 shows initial voltage waveforms of energization overvoltages of the OHL when the source impedance is 100 mH. It demonstrates that the line length 96 km leads to the highest overvoltage as expected. This was, however, not observed in [5] since the source impedance 100 mH was not the study condition that leads to the maximum overvoltage. That is, the study condition 100 mH and 96 km caused a lower overvoltage than 30 mH and 96 km.

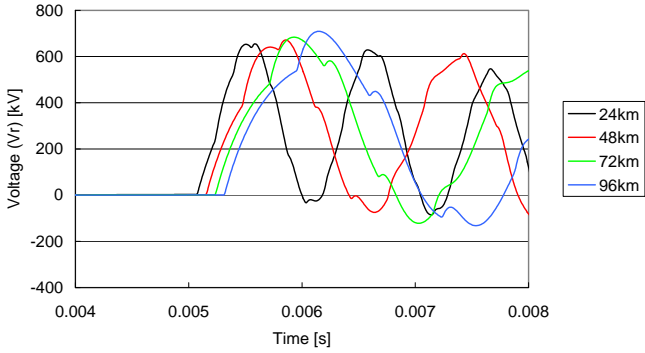


Fig. 7 Initial voltage waveforms of the energization overvoltage for the OHL (source impedance: 100 mH).

Fig. 8 shows initial voltage waveforms of energization overvoltages of the cable at the receiving end ( $V_r$ ). The source impedance is set to 1 mH since the maximum overvoltage was observed with the source impedance 1 mH. As the source impedance is set so small, not only the rate of voltage rise but also the magnitude of the overvoltage becomes larger, compared with other source impedance values.

Another significant difference from other source impedance values is how the coaxial mode is reflected at the sending end. With the source impedance 1 mH, the reflection at the sending end is negative reflection, whereas the reflection at the sending end is positive reflection with other source impedance values. It is because the voltage level at the sending end is fixed to the source voltage when the source impedance is 1 mH.

The difference in the reflections can be clearly observed in Fig. 8. So far, the superimposition of the two modes raised the highest overvoltage. On the contrary, in Fig. 8, the negative coaxial mode (2nd wave) makes dents on the peaks of the inter-phase mode (1st wave). The inter-phase mode (1st wave) is larger for shorter line lengths, but the negative coaxial mode (2nd wave) is also larger for shorter line lengths. As a result, the highest overvoltage is observed in case of the line length 48 km, and the effect of the line length on the highest overvoltage is reduced.

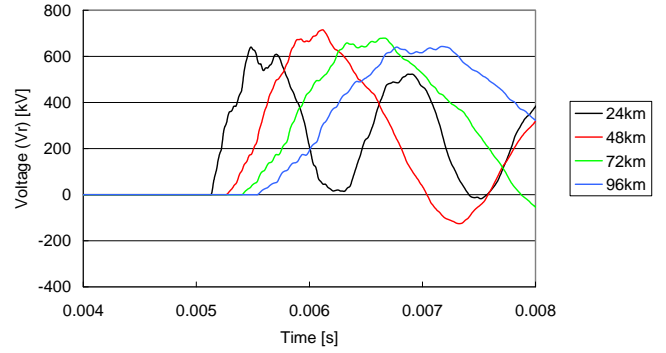


Fig. 8 Initial voltage waveforms of the energization overvoltage for the cable (source impedance: 1 mH).

Fig. 9 and Fig. 10 compare initial voltage waveforms of energization overvoltages of the cable for source impedances 30 mH and 100 mH.

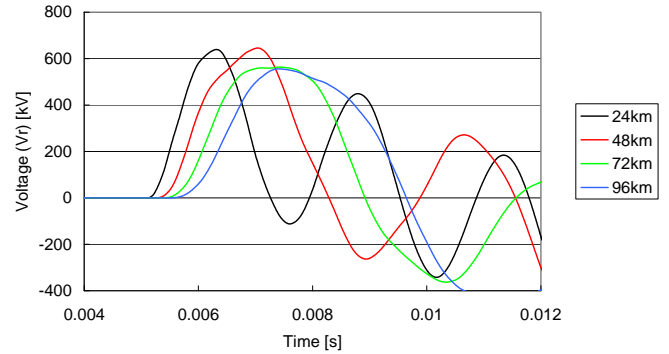


Fig. 9 Initial voltage waveforms of the energization overvoltage for the cable (source impedance: 30 mH).

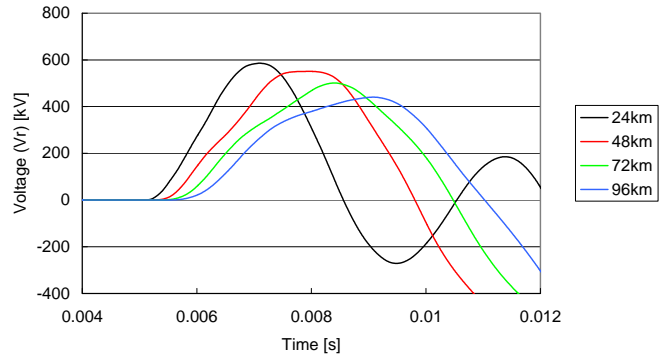


Fig. 10 Initial voltage waveforms of the energization overvoltage for the cable (source impedance: 100 mH).

With the source impedances 30 mH and 100 mH, shorter line lengths lead to higher overvoltages as expected. This characteristic was, however, not observed in [5] since the source impedance 30 mH or 100 mH was not the study condition that leads to the maximum overvoltage. The negative coaxial mode is not observed in these cases.

As we found in the last section, the cycle time of the dominant mode of the cable is long (3.85 ms) with the line length 48 km and the source impedance 30 mH. It becomes even longer for longer line lengths or larger source

impedances. As such, the horizontal axis of Fig. 9 and Fig. 10 is extended from 8 ms to 12 ms. The cable is energized at the voltage peak of phase a (5 ms), but the source voltage goes down to zero at 10 ms. This also contributes to lower overvoltages in case of longer line lengths or larger source impedances.

## V. ANALYSIS ON THE EFFECTS OF FEEDING NETWORK

This section studies why energization overvoltages for cables become lower for a larger source impedance while those for OHLs peak with the source impedance 30 mH.

Fig. 11 shows initial voltage waveforms of energization overvoltages of the OHL at the receiving end ( $V_r$ ). The switch timing is set to 5 ms as in the previous sections. The line length is set to 72 km since the maximum overvoltage was observed with the source impedance 72 km.

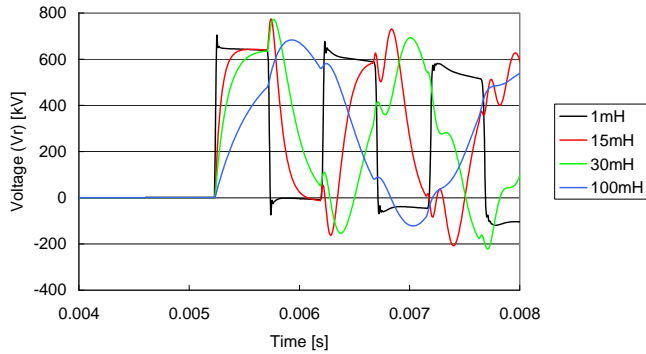


Fig. 11 Initial voltage waveforms of the energization overvoltage for the OHL (line length: 72 km).

As discussed in the last section, the highest overvoltage of the OHL is determined by the timing when the earth-return mode reaches its maximum and the inter-phase mode arrives at the receiving end. Fig. 11 shows that source impedances 15 mH and 30 mH have the timing to cause high overvoltages. When the source impedance is 1 mH, the overvoltage of the inter-phase mode is smaller, which results in the lower overvoltage.

Fig. 12 and Fig. 13 show initial voltage waveforms of energization overvoltages of the cable for line lengths 24 km and 48 km. These two lengths were selected as we learned in the last section that shorter line lengths lead to higher overvoltages except when the source impedance is 1 mH.

Fig. 12 demonstrates that smaller source impedances lead to larger overvoltages as we found in [5]. This is not true only when the source impedance is 1 mH.

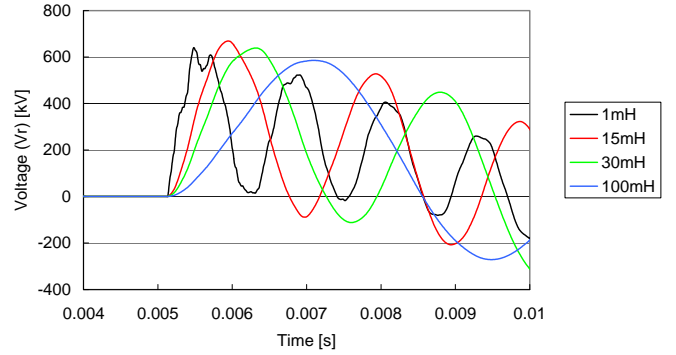


Fig. 12 Initial voltage waveforms of the energization overvoltage for the cable (line length: 24 km).

When the source impedance is 1 mH, the highest overvoltage is caused when the line length is 48 km as we learned in the last section. Looking at the source impedance 1 mH in Fig. 13 and other source impedances in Fig. 12, it is clear that smaller source impedances lead to larger overvoltages.

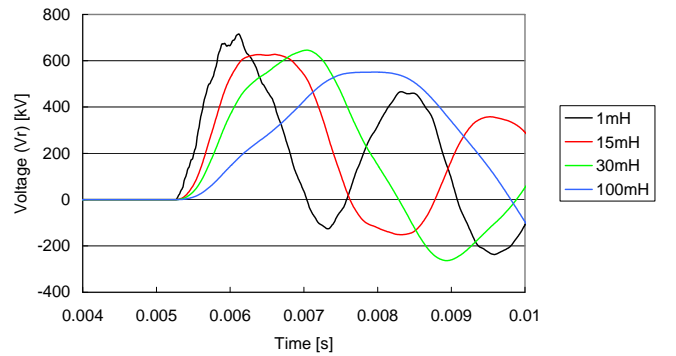


Fig. 13 Initial voltage waveforms of the energization overvoltage for the cable (line length: 48 km).

It is reasonable to have larger overvoltages with smaller source impedances as the rate of voltage rise becomes larger for smaller source impedances. The larger rate of voltage rise is apparent as the smaller source impedances lead to a higher dominant frequency contained in the energization overvoltage. For larger source impedances, due to their slow rates of voltage rise, the fundamental component already starts to decrease from the voltage peak by the time when the inter-phase mode reaches its maximum.

## VI. CONCLUSION

This paper analyzed the characteristics of the energization overvoltage observed in [5]. The analysis has found that these characteristics are not caused by random switching by accident. Rather, there are contributing factors and physical meanings behind the characteristics.

In summary, the analysis has identified contributing factors and has explained their physical meanings as follows:

- Energization overvoltages for cables are lower than those

for OHLs because the overvoltage of the coaxial mode in cables is smaller and more obtuse, compared with the inter-phase mode in OHLs. The long cycle time of the inter-phase mode in cables also affects this characteristic.

- Energization overvoltages for cables do not show any dependence on the line length because the maximum overvoltages are observed with the source impedance 1 mH. The negative coaxial mode makes dents on the peaks of the maximum overvoltage when the source impedance is 1 mH. With the other source impedances, shorter line lengths lead to higher overvoltages.
- Energization overvoltages for cables become lower for larger source impedances, which is reasonable from the theoretical analysis.
- Highest energization overvoltages for OHLs are caused by the superimposition of the inter-phase mode on the earth-return mode. The timing of the superimposition determines the magnitude of the highest overvoltage, and the line length and the source impedance affect this timing. The energization overvoltage for OHLs peak with the line length 72 km and the source impedance 30 mH because the combination provided the best timing for the superimposition within the studied conditions.

Since the contributing factors and physical meanings of the characteristics have been identified, it is now possible to use the obtained statistical distribution for the determination of insulation levels of cable systems. Especially, the obtained statistical distribution suggests a possible application of lower insulation levels to cable systems compared with OHLs. However, it may present a future challenge to define insulation levels for temporary overvoltages since a possibility of severe temporary overvoltages are reported in relation to cable systems [9]-[12].

## VII. REFERENCES

- [1] CIGRE Working Group 13.02, "Switching Overvoltages in EHV and UHV Systems with Special Reference to Closing and Reclosing Transmission Lines," *Electra N°30*, pp. 70-122, 1973.
- [2] CIGRE Working Group 13.05, "The Calculation of Switching Surges," *Electra N°19*, pp. 67-78, 1971.
- [3] CIGRE Working Group 13.05, "The Calculation of Switching Surges – II. Network Representation for Energization and Re-energization Studies on Lines Fed by an Inductive Source," *Electra N°32*, pp. 17-42, 1974.
- [4] CIGRE Working Group 13.05, "The Calculation of Switching Surges – III. Transmission Line Representation for Energization and Re-energization Studies with Complex Feeding Networks," *Electra N°62*, pp. 45-78, 1979.
- [5] T. Ohno, C. L. Bak, A. Ametani, W. Wiechowski, and T. K. Sørensen, "Statistical Distribution of Energization Overvoltages of EHV cables," *IEEE Trans. on Power Delivery*, (under publication process).
- [6] A. Morched, B. Gustavsen, M. Tartibi, "A Universal Line Model for Accurate Calculation of Electromagnetic Transients on Overhead Lines and Cables," *IEEE Trans. on Power Delivery*, vol. 14, no. 3, 1999, pp. 1032–1038.
- [7] Bjørn Gustavsen "Panel Session on Data for Modeling System Transients. Insulated Cables", *Proc. IEEE. Power Engineering Soc. Winter Meeting*, 2001.
- [8] A. Ametani, Y. Miyamoto, N. Nagaoka, "An Investigation of a Wave Propagation Characteristic on a Crossbonded Cable", *IEEJ Transaction B*, vol. 123, no. 3, 2003 (in Japanese).
- [9] T. Karasaki, T. Goto, A. Ametani, "An Abnormal Overvoltage due to Load Rejection on EHV Underground Transmission Lines", *International Conference on Power System Transients (IPST)*, September 1995.
- [10] N. Momose, H. Suzuki, S. Tsuchiya, T. Watanabe, "Planning and Development of 500 kV Underground Transmission System in Tokyo Metropolitan Area", *CIGRE Session 37-202*, 1998.
- [11] L. Colla, M. Rebolini, F. Illiceto, "400 kV AC new submarine cable links between Sicily and the Italian mainland. Outline of project and special electrical studies", *CIGRE Session C4-116*, 2008.
- [12] *Assessment of the Technical Issues relating to Significant Amounts of EHV Underground Cable in the All-island Electricity Transmission System*, (available on the web) Tokyo Electric Power Company, November 2009, <http://www.eirgrid.com/media/Tepco%20Report.pdf>.